

Polymer Chemistry

Accepted Manuscript



This is an *Accepted Manuscript*, which has been through the Royal Society of Chemistry peer review process and has been accepted for publication.

Accepted Manuscripts are published online shortly after acceptance, before technical editing, formatting and proof reading. Using this free service, authors can make their results available to the community, in citable form, before we publish the edited article. We will replace this *Accepted Manuscript* with the edited and formatted *Advance Article* as soon as it is available.

You can find more information about *Accepted Manuscripts* in the [Information for Authors](#).

Please note that technical editing may introduce minor changes to the text and/or graphics, which may alter content. The journal's standard [Terms & Conditions](#) and the [Ethical guidelines](#) still apply. In no event shall the Royal Society of Chemistry be held responsible for any errors or omissions in this *Accepted Manuscript* or any consequences arising from the use of any information it contains.

ARTICLE

Organo-Photocatalysts for Photoinduced Electron Transfer – Reversible Addition-Fragmentation Chain Transfer (PET-RAFT) Polymerization

Cite this: DOI: 10.1039/x0xx00000x

Jiangtao Xu,^{*} Sivaprakash Shanmugam, Hien T. Duong and Cyrille Boyer^{*}Received 00th January 2012,
Accepted 00th January 2012

DOI: 10.1039/x0xx00000x

www.rsc.org/

ABSTRACT: In this article, we are investigating a series of organo-dyes, including methylene blue, fluorescein, rhodamine 6G, Nile red and eosin Y, to perform a visible light-mediated controlled/“living” radical polymerization of methacrylates. We demonstrate that eosin Y and fluorescein were efficient catalysts to activate a photoinduced electron transfer-reversible addition-fragmentation chain transfer (PET-RAFT) mechanism. The concentration of eosin Y was varied from 10-100ppm in respect to monomer. This polymerization technique yielded well-defined (co)polymers with a good control of the molecular weights ranging from 10,000 to 100,000 g/mol and low polydispersities (PDI < 1.30). A variety of functional monomers, including *N,N*-dimethylaminoethyl methacrylate, hydroxyl ethyl methacrylate, pentafluorophenyl methacrylate, glycidyl methacrylate, oligoethylene glycol methyl ether methacrylate (OEGMA), methacrylic acid were successfully polymerized. Finally, the addition of tertiary amine, such as triethylamine, afforded to carry out the polymerization in the presence of air via a reductive quenching cycle. Different diblock polymethacrylate copolymers, i.e. PMMA-*b*-POEGMA and PMMA-*b*-PMMA, were prepared to demonstrate the high end group fidelity.

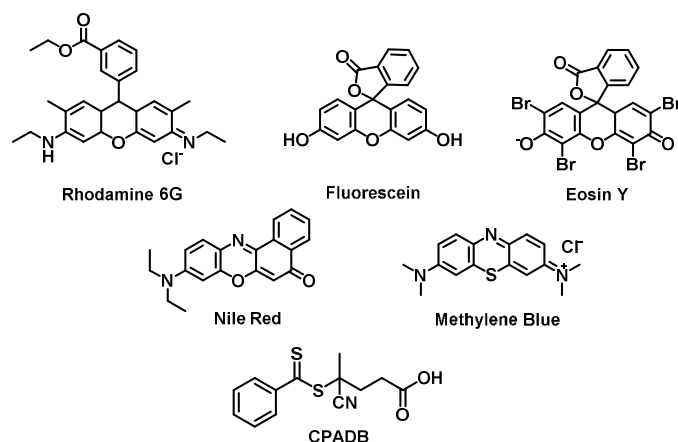
KEYWORDS: Controlled/living radical polymerization, photoinduced electron transfer, reversible addition-fragmentation chain transfer and organo-photoredox catalyst

INTRODUCTION:

Polymerization regulated by visible light is considered to be eco-friendly and a sustainable alternative to traditional thermal initiated polymerization, along with a variety of attractive features, including simple experimental setup, mild reaction conditions, minimal side reactions and spatio-temporal control.¹⁻³ Visible light photoredox catalysis employed for controlled/“living” radical polymerization, now referred to as reversible deactivation radical polymerization (RDRP), is an emerging topic attracting significant interests in polymer and material chemistry, since 2010.⁴⁻¹⁵ For instance, Hawker and Fors employed for the first time a photo-redox catalyst based on iridium catalyst to activate an atom transfer radical polymerization-like process under visible light.^{4, 5, 16} This process was inspired by the seminal works of MacMillan,¹⁷⁻¹⁹ Stephenson²⁰⁻²² and Yoon^{19, 23} in organic synthesis. In these reactions, the photoredox catalyst plays a crucial role in terms of durability, applicability and reactivity for visible light

photoredox reactions. The most popular catalysts are transition metal complexes due to their strong light absorption, long excited state lifetime and high stability.¹⁸ However, they are expensive and potentially toxic, which limits their implementation or commercialization.²⁴ Recently, organo-photocatalysts have emerged as an alternative to these metallic based catalysts due to their low costs, availability and low toxicity.²⁵ Organic dyes with diverse absorption were proven to be highly efficient in photoredox catalysis for synthetic transformations in organic synthesis.^{26, 27} For instance, Eosin Y (EY, **Scheme 1**) is one of the widely used organic dyes, commonly employed as a biological stain for fluorescence studies of cytoplasm, collagen and muscle fibre.²⁸ Its photochemistry has also been well investigated.^{24, 29} Upon excitation by visible light, EY rapidly undergoes intersystem crossing from singlet excited state to the lowest energy triplet excited state, which has a lifetime of 24μs.^{24-26, 30} The triplet state of EY has strong reducing ($E^*_{\text{red}}(\text{PC}^{\bullet}/\text{PC}^{\bullet}) = +1.18 \text{ V vs SCE}$) and oxidizing ($E^*_{\text{red}}(\text{PC}^{\bullet}/\text{PC}^{\bullet}) = -1.60 \text{ V vs SCE}$)

potentials, which was successfully employed in organic transformations to substitute metal-based catalyst.^{24, 31} Finally, EY has also been successfully employed to mediate free radical polymerization in the presence of tertiary amine, such as methyldiethanolamine, and *N*-vinylpyrrolidone.³²⁻³⁵ Recently, we developed a versatile and robust photoinduced living polymerization technique, named photoinduced electron transfer – reversible addition–fragmentation chain transfer (PET-RAFT) polymerization,³⁶⁻³⁸ which is capable of polymerizing a large range of conjugated and unconjugated monomers to afford polymers with well-defined structures and narrow polydispersities, even in the presence of air and ultra-low concentration of catalyst. In this process, a photocatalyst, such as *fac*-[Ir(ppy)₃] and Ru(bpy)₃Cl₂, activates RAFT polymerization by an electron transfer between the catalyst and RAFT agent. Based on our previously reported mechanism of PET-RAFT, we envisaged that organo-dyes have the potential to be effective photoredox catalysts. In this paper, we investigated a series of organo-dyes, including EY, methylene blue, fluorescein, Nile red, and rhodamine 6G, which were commonly employed in organic synthesis. These dyes would be ideal organo-photocatalyst for controlled/“living” polymerization as they are non-toxic (commonly employed in biology, as staining agent for confocal microscopy).



Scheme 1. Chemical structures of organo-dyes and CPADB employed in this study.

In this article, we demonstrate for the first time, the applicability of organo-dyes for the activation of PET-RAFT mechanism to afford the preparation of well-defined polymethacrylates and their block copolymers. Most importantly, this polymerization technique is tolerant of diverse functionalities and oxygen; and can be performed in various organic solvents and water.

EXPERIMENTAL

Materials

Methyl methacrylate (MMA, 99%), *tert*-butyl methacrylate (*t*BuMA, 99%), *tert*-butyl acrylate (*t*BuA, 99%), oligo (ethylene glycol) methyl ether methacrylate (OEGMA, average M_n 300), methylene blue (95%), fluorescein (95%), rhodamine

6G (99%), Nile red (98%), Eosin Y (EY, 99%), and triethylamine ($\geq 99\%$) were all purchased from Sigma-Aldrich. Deinhhibition of monomers was performed by percolating over a column of basic alumina (Ajax Chemical, AR). Dimethyl sulfoxide (DMSO), acetonitrile (MeCN), toluene, and *N,N*-dimethylformamide (DMF), diethyl ether, and petroleum spirit were purchased from Ajax Chemical and used as received. 4-cyanopentanoic acid dithiobenzoate (CPADB) was prepared according to the literature.^{39, 40}

Instrumentation

Gel permeation chromatography (GPC) was performed using tetrahydrofuran (THF) or dimethylacetamide (DMAc) as the eluent. The GPC system was a Shimadzu modular system comprising an auto injector, a Phenomenex 5.0 μ m beads size guard column (50 \times 7.5mm) followed by four Phenomenex 5.0 μ m bead-size columns (10⁵, 10⁴, 10³ and 10² Å) for DMAc system, two MIX C columns provided by Polymer Lab for THF system, and a differential refractive-index detector and a UV detector. The system was calibrated with narrow molecular weight distribution polystyrene standards with molecular weights of 200 to 10⁶ g mol⁻¹.

Nuclear Magnetic Resonance (NMR) spectroscopy was carried out on a Bruker Advance III with SampleXpress operating at 300MHz for ¹H using CDCl₃ as solvent and tetramethylsilane (TMS) as a reference. The data obtained was reported as chemical shift (δ) measured in ppm downfield from TMS.

UV-vis Spectroscopy spectra were recorded using a CARY 300 spectrophotometer (Varian) equipped with a temperature controller.

On-line Fourier Transform Near-Infrared (FTNIR) spectroscopy was used to measure the monomer conversions by following the decrement of the vinylic C-H stretching overtone of the monomer at $\sim 6,200\text{cm}^{-1}$. A Bruker IFS 66/S Fourier transform spectrometer equipped with a tungsten halogen lamp, a CaF₂ beam splitter and liquid nitrogen cooled InSb detector was used. The sample was placed in a FTNIR quartz cuvette (1cm \times 2mm) and polymerised under blue LED light irradiation ($\lambda_{\text{max}} = 435\text{nm}$). Every 5, 10, or 30 minutes, the sample was put into a holder manually and each spectrum in the spectral region of 7,000-5,000 cm^{-1} was constructed from 32 scans with a resolution of 4 cm^{-1} . The total collection time per spectrum was about 15 s. Spectra were analysed with OPUS software.

Photopolymerization reactions were carried out in the same reaction vessel used in our previous work,³⁷ where the reaction mixtures were irradiated by one meter of blue LED strip (4.8 W, $\lambda_{\text{max}} = 435\text{nm}$).

Synthetic procedures

General procedure for the kinetic studies of PET-RAFT polymerization of methyl methacrylate (MMA) mediated by different dyes in the absence of oxygen. As an example of MMA polymerization by fluorescein at 500 ppm (relative to monomer) catalyst concentration, a reaction solution consisting of DMSO (1mL), MMA (0.94g, 9.4mmol), CPADB (13.1mg,

0.047mmol) and fluorescein (1.56mg, 4.7×10^{-3} mmol) was prepared in a 4mL glass vial. Sealed with a rubber septum and covered with aluminium foil the reaction solution was degassed for 20 minutes with N_2 and then irradiated under blue LED light (4.8 W, $\lambda_{\max} = 435\text{nm}$) at room temperature. After 24 h, the monomer conversions and molecular weight were analysed by ^1H NMR (CDCl_3) and GPC (RI and UV detectors).

For the polymerization mediated by methylene blue, the reaction solutions were irradiated by both blue and red LED ($\lambda_{\max} = 635\text{ nm}$) lights. In the case of Nile red, the light sources were blue and green LED ($\lambda_{\max} = 530\text{ nm}$). The reaction setup referred to supporting information.

General procedure for the kinetic studies of PET-RAFT polymerization of methyl methacrylate (MMA) mediated by Eosin Y (EY) by on-line Fourier transform near-Infrared (FTNIR) spectroscopy in the absence and presence of oxygen. A reaction stock solution consisting of DMSO (1mL), MMA (0.94g, 9.4mmol), CPADB (13.1mg, 0.047mmol) and eosin Y (0.61mg, 9.4×10^{-4} mmol) was prepared in a 4mL glass vial. 0.7mL of this stock solution was transferred into a 0.9mL FTNIR quartz cuvette (1cm \times 2mm). To examine the polymerization in the absence of oxygen the cuvette was sealed with a rubber septum and covered with aluminium foil while degassing for 20 minutes with N_2 . The quartz cuvette was then irradiated under blue LED light (4.8 W, $\lambda_{\max} = 435\text{nm}$) at room temperature. The cuvette was transferred to the sample holder manually for FTNIR measurement every 30 minutes. After 15 seconds scanning, the cuvette was moved back into light. The monomer conversions were calculated by the ratio of the integral of the wavenumber area $6220 \sim 6120\text{cm}^{-1}$ at different time points to that at 0 minute. Aliquots of the final reaction mixtures were analysed by ^1H NMR (CDCl_3) and GPC (RI and UV detectors) to measure the conversions, number average molecular weights ($M_{n, \text{GPC}}$), and polydispersities (M_w/M_n). The remainder was purified *via* precipitation in methanol/petroleum ether (1/1, v/v). The final pink powder was collected and submitted for UV-vis spectroscopy and ^1H NMR measurements to confirm chain end group fidelities and calculate absolute molecular weights, $M_{n, \text{NMR}}$.

$$M_{n, \text{NMR}} = (I^{3.6\text{ppm}}/3)/(I^{7.8\text{ppm}}/2) \times MW^{\text{MMA}} + MW^{\text{CPADB}}$$

Where $I^{3.6\text{ppm}}$ and $I^{7.8\text{ppm}}$ correspond to integrals of peak signal at δ 3.6ppm and δ 7.8ppm attributed to OCH_3 of MMA and phenyl group of CPADB, respectively.

To examine the polymerization in the presence of oxygen, another 0.7mL aliquot of the stock solution was polymerized and analysed using an identical procedure except for elimination of the degassing step.

General procedure for the kinetic studies of PET-RAFT polymerization of methyl methacrylate (MMA) mediated by eosin Y/triethylamine (EY/TEA) by on-line Fourier transform near-Infrared (FTNIR) spectroscopy in the absence and presence of oxygen.

A reaction stock solution consisting of DMSO (1mL), MMA (0.94g, 9.4mmol), CPADB (13.1mg, 0.047mmol), eosin Y (0.61mg, 9.4×10^{-4} mmol) and TEA (mg, 4.76mg, 0.047mmol) was prepared in a 4mL glass vial. 0.7mL of this stock solution

was transferred into a 0.9mL FTNIR quartz cuvette (1cm \times 2mm). To examine the polymerization in the presence of oxygen the cuvette was sealed with a rubber septum. The quartz cuvette was then irradiated under blue LED light (4.8W, $\lambda_{\max} = 435\text{nm}$) at room temperature. The cuvette was transferred to the sample holder manually for FTNIR measurement every 30 minutes. After 15 seconds scanning, the cuvette was moved back into light. The monomer conversions were calculated by the ratio of the integral of the wavenumber area $6220 \sim 6120\text{cm}^{-1}$ at different time points to that at 0minute. Aliquots of the final reaction mixtures were analysed by ^1H NMR (CDCl_3) and GPC (RI and UV detectors) to measure the conversions, number average molecular weights ($M_{n, \text{GPC}}$), and polydispersities (M_w/M_n). The remainder was purified *via* precipitation in methanol/petroleum ether (1/1, v/v). The final pink powder was collected and submitted for UV-vis spectroscopy and ^1H NMR measurements to confirm chain end group fidelities and calculate absolute molecular weights, $M_{n, \text{NMR}}$.

To examine the polymerization in the absence of oxygen, another 0.7mL aliquot of the stock solution was degassed with nitrogen for 20 minutes, and then polymerized and analysed using an identical procedure.

General procedure for PET-RAFT polymerization of functional monomers mediated by EY in the absence of oxygen. In a typical experiment synthesizing poly(2-hydroxyethyl methacrylate) (PHEMA), a 5mL glass vial was equipped with a rubber septum and charged with DMSO (0.5mL), HEMA (1.41g, 14.1mmol), CPADB (20mg, 0.0705mmol), eosin Y (0.46mg, 7.05×10^{-4} mmol). The mixture was covered with aluminium foil while degassing for 20 minutes with N_2 . The reaction mixture was then irradiated under a blue LED light at room temperature for 21 hours. The final solution was precipitated in diethyl ether by stirring. The pink precipitate was collected, re-dissolved in a minimal amount of dichloromethane, and precipitated a second time from diethyl ether. The pink precipitate was then collected and dried to yield the desired product.

General procedure for the preparation of diblock copolymers by PET-RAFT polymerization mediated by EY/TEA in the presence of oxygen. In a typical experiment synthesizing the diblock copolymer poly(methyl methacrylate)-*b*-poly(methylmethacrylate) (PMMA-*b*-PMMA), a 5mL glass vial was equipped with a rubber septum and charged with DMSO (1.5mL), MMA (1.41g, 14.1mmol), CPADB (20mg, 0.0705mmol), eosin Y (0.46mg, 7.05×10^{-4} mmol), and TEA (7.1mg, 0.0705mmol). The mixture was then irradiated under a blue LED light at room temperature for 21 hours. The final solution was precipitated in mixture of methanol/petroleum spirit (1/1, v/v) with stirring. The pink precipitate was collected, re-dissolved in a minimal amount of dichloromethane, and precipitated a second time from the mixture of methanol/petroleum spirit (1/1, v/v). The pink precipitate was then collected and dried to yield the desired product: $M_{n, \text{GPC}} = 21\,710\text{ g/mol}$, $M_w/M_n = 1.09$.

For the chain extension, a 5mL glass vial was equipped with a rubber septum and charged with DMSO (0.5mL), MMA (0.076g, 0.76mmol), PMMA macro-initiator (0.08g, $M_n = 21,270\text{g/mol}$, 0.0038mmol), eosin Y (0.025mg, $3.8 \times 10^{-5}\text{mmol}$) and TEA (0.38g, 0.0038mmol). The mixture was then irradiated under a blue LED light at room temperature for 13 hours. The final solution was precipitated in methanol with stirring. The pink precipitate was collected, re-dissolved in a minimal amount of dichloromethane, and precipitated a second time from methanol. The pink precipitate was then collected and dried to yield desired product: $M_{n,\text{GPC}} = 33,200\text{g/mol}$, $M_w/M_n = 1.13$.

RESULTS AND DISCUSSION

Initial polymerizations of methyl methacrylate (MMA) were investigated using CPADB as chain transfer agent in the presence of organic photo-redox catalysts (500ppm relative to monomer) under blue LED light ($\lambda_{\text{max}} = 435\text{ nm}$, 4.8W). We tested different organo-dyes, including EY, fluorescein, Nile red, methylene blue, and rhodamine 6G due to their low redox potentials. After 24 hours of polymerization, the monomer conversions were determined by NMR for the different dyes. Encouraging results were noted for EY and fluorescein where monomer conversions greater than 50% were observed, while in the case of other dyes, the monomer conversion was less than 10% (or not detectable by NMR) which was attributed to self-initiation of MMA under blue LED light (**Table 1**). According to our data, we can rank the organo-photoredox catalyst by order of reactivity to activate PET-RAFT: eosin Y >> fluorescein >> Nile red, rhodamine and methylene blue.

Table 1. PET-RAFT polymerization tests of MMA with various organo-dyes in the absence of oxygen under blue LED light (435 nm, 5 W).

Organo-dye	[MMA]/[CPADB]/[catalyst]	T (h)	α^M (%) ^a	$M_{n,\text{th}}$ ^b	$M_{n,\text{exp}}$ ^c	PDI ^e
Fluorescein	200 : 1 : 0.1	24	51.2	11 520	12 160	1.18
Eosin Y	200 : 1 : 0.02	24	92.4	18 100	18 700	1.23
Methylene Blue ^d	200 : 1 : 0.1	24	0	-	-	-
Nile Red ^e	200 : 1 : 0.1	24	0	-	-	-
Rhodamine 6G	200 : 1 : 0.1	24	10	2 420	4 250	1.13

Note: a) Monomer conversion determined by ¹H NMR spectroscopy using the following equation: $\alpha^M = [(5.5-6.0\text{ppm})/2]/[(3.5\text{ppm}/3)]$, b) theoretical molecular weight calculated using $M_{n,\text{th}} = ([\text{MMA}]/[\text{CPADB}]) \times \alpha^M \times \text{MW}^{\text{MMA}} + \text{MW}^{\text{CPADB}}$, c) experimental molecular weight and polydispersity (PDI) determined by THF GPC using universal calibration; d) Polymerizations were conducted under both blue and red ($\lambda_{\text{max}} = 635\text{ nm}$) LED light; e) Polymerizations were conducted under both blue ($\lambda_{\text{max}} = 435\text{ nm}$) and green ($\lambda_{\text{max}} = 530\text{ nm}$) LED lights.

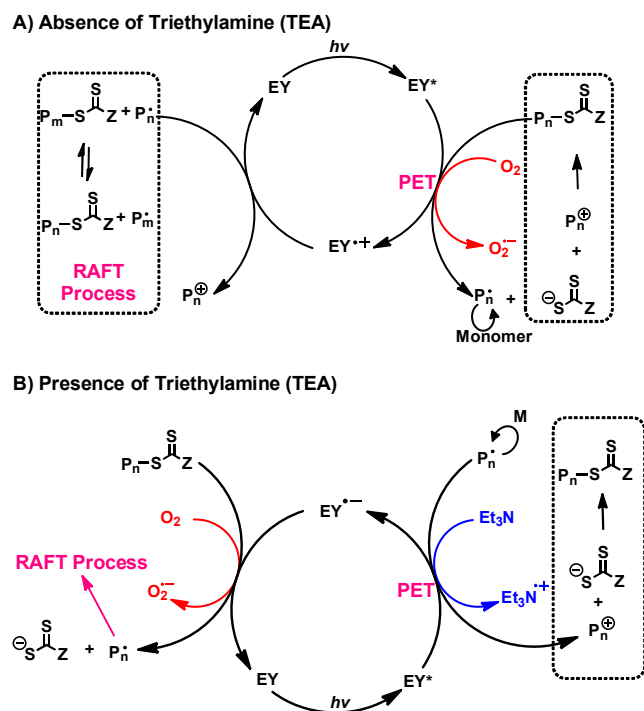
On the basis of our previous research using iridium and ruthenium catalysts,³⁶⁻³⁷ we preliminarily propose the following criteria must be met to have an effective photoredox catalyst: (a) it must have a lower reduction potential $E_{\text{red}}^*(\text{PC}^{\bullet+}/\text{PC}^*)$ than that of RAFT agents; (b) it should exhibit a low quantum

yield for fluorescence; (c) it should have a fairly high intersystem crossing rate. EY presents the longest excitation lifetime in comparison to other organo-dyes investigated in this study and present the lowest fluorescence quantum yield ($\Phi = 0.47$, **Table 1**).⁴¹⁻⁴⁴ A low value of quantum yield reveals that significant energy received by the dye is wasted in thermal dissipation and other energy transfers, while a high fluorescence quantum yield corresponds to high conversion of energy into fluorescence. In addition, the reduction potential of EY ($E_{\text{red}}^*(\text{PC}^{\bullet+}/\text{PC}^*)$) is much lower than that of the RAFT agent [$E_{\text{red}}^*(\text{CPADB}/\text{CPADB}^{\bullet-}) \sim -0.4\text{ V}$],³⁶ which allows activation of PET process. Therefore methylene blue with higher reduction potential (+0.01V) cannot initiate the polymerization. Although fluorescein is a stronger reducing agent [$E_{\text{red}}^*(\text{PC}^{\bullet+}/\text{PC}^*) = -1.22\text{ V}$] than EY, fluorescein presents a higher fluorescence quantum yield ($\Phi = 0.95$) than EY ($\Phi = 0.57$). The decrease in fluorescence of EY (compared to fluorescein) is predominantly due to an increase in intersystem crossing⁴¹ which allows EY to be in the excited state for a longer time (24 μs) than fluorescein and by consequence dissipated the energy via other processes like electron transfer.^{24, 42} In our experiments, we show that polymerization is activated when fluorescein concentration is equal to 500ppm relative to monomer concentration. Rhodamine 6G has also a reduction potential [$E_{\text{red}}^*(\text{PC}^{\bullet+}/\text{PC}^*) \sim -0.8\text{ V vs SCE}$]⁴³ comparable to RAFT agent [$E_{\text{red}}^*(\text{CPADB}/\text{CPADB}^{\bullet-}) \sim -0.4\text{ V}$] with a very high fluorescence quantum yield ($\Phi > 0.95$).⁴⁴ Thus it cannot activate the PET-RAFT process. In the case of Nile red, the low quantum yield observed in DMSO (or polar solvents) are due to the aggregation of the hydrophobic benzophenoxazinone core structures.⁵⁴ In addition, Nile red is also a good radical scavenger.⁵⁵

Table 2. Properties of dyes.⁴¹⁻⁴⁴

Organo-dye	$E_{\text{red}}^*(\text{PC}^{\bullet+}/\text{PC}^*)$	Φ^b	k_r^c (ns ⁻¹)	k_{nr}^d (ns ⁻¹)
Fluorescein	-1.22 V	0.95	1.61	1.4
Eosin Y	-1.1 V	0.47	1.40	56.1
Methylene Blue	+0.01 V	> 0.55	-	-
Nile Red	-1.02 V	0.71	-	-
Rhodamine 6G	-0.8 V	0.95	0.221	0.025

Note: a) Reduction potential in V vs SCE; b) quantum yield, c) radiative decay constant (ns⁻¹); d) Non-radiative constant (ns⁻¹).



Scheme 2. Proposed mechanisms for PET-RAFT polymerization mediated by eosin Y in the absence (A, oxidative quenching cycle) and presence (B, reductive quenching cycle) of sacrificial electron donor, triethylamine (TEA), and their oxygen tolerance.

After these initial results, EY was selected and investigated in detail. Several control experiments (no.1-3, **Table 3**) were carried out to investigate possible side reactions. The radical polymerization of MMA could not proceed successfully to achieve high monomer conversion (< 10% in all cases) after 24 hours of light irradiation in the absence of chain transfer agent, i.e. CPADB, or catalyst, i.e. EY. This suggested that CPADB and EY were key components in this polymerization process. Previous studies demonstrated that EY can absorb light to yield excited EY*, which is capable of transferring an electron by photo-induced electron transfer (PET). CPADB accepts the electron and acts as initiator as well as chain transfer agent to mediate chain growth in a living manner (**Scheme 2A**).

The kinetic study and “ON/OFF” experiment of MMA photopolymerization in the absence of oxygen was carefully investigated. As shown in **Figure S1**, ESI, temporal control of the polymerization was clearly demonstrated by the light “ON” and “OFF” switch on the plot of $\ln([M]_0/[M]_t)$ (derived from conversion measured by online Fourier transfer near-Infrared (FTNIR) spectroscopy) versus time. The polymerization system remained dormant with no polymerization taking place in the absence of light, when the light was back “ON”; the system was activated and resumed polymerizing. These “activation” and “deactivation” processes were easily manipulated by controlling “ON” and “OFF” periods.

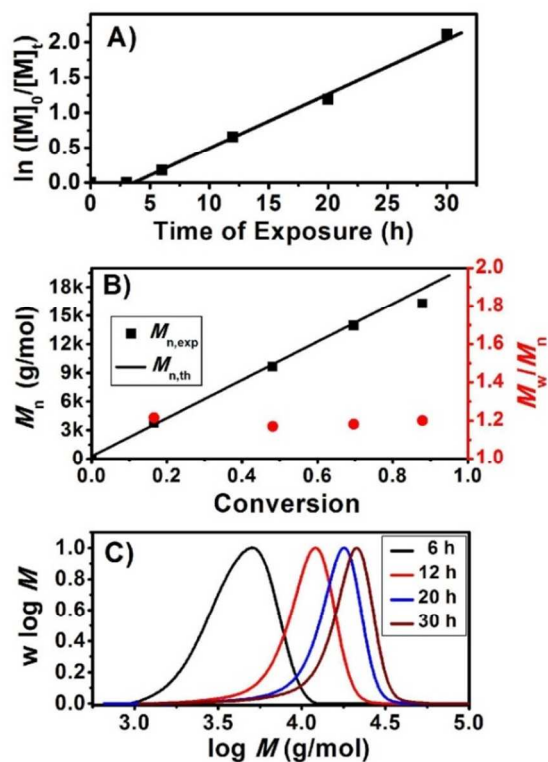
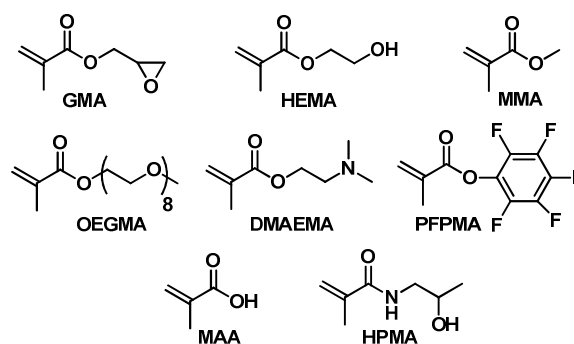


Figure 1. PET-RAFT polymerization of MMA mediated by eosin Y (EY) in DMSO using CPADB as thiocarbonylthio compound: A) $\ln([M]_0/[M]_t)$ vs. time of exposure; B) molecular weights and M_w/M_n vs. conversion; C) molecular weight distributions of PMMA at different time points. Note: The reactions were performed in DMSO at room temperature under 4.8 W blue LED light ($\lambda_{\max} = 435$ nm) using $[MMA]:[CPADB]:[EY] = 200 : 1 : 0.02$ in the absence of oxygen.

Linear plot of $\ln([M]_0/[M]_t)$ versus exposure time (**Figure 1A**) suggested that constant concentration of propagating free radicals were achieved during the polymerization period, although three hours induction period was observed. The evolution of experimental molecular weights to monomer conversion showed a linear evolution with an excellent agreement to theoretical molecular weights (**Figure 1B**), which was in accord with a controlled/“living” polymerization behaviour. Monomodal distributions of molecular weights with a clear shift with exposure time (**Figure 1C**) and narrow polydispersities (M_w/M_n) lower than 1.2, indicated a good control of the polymerization.

After demonstrating that EY can activate PET-RAFT polymerization, we decided to test the versatility of this approach for the polymerization of functional monomers, including hydroxyethyl methacrylate (HEMA), *N,N*-dimethylaminoethyl methacrylate (DMAEMA), glycidyl methacrylate (GMA), hydroxypropyl methacrylamide (HPMA), methacrylic acid (MAA), pentafluorophenyl methacrylate (PFPMMA) and oligoethylene glycol methyl ether methacrylate (OEGMA). **Table 4** summarizes the various polymers prepared in this study. In contrast, to our previous studies using *fac*-[Ir(ppy)₃], functional monomers, such as DMAEMA and GMA, were not well controlled with a PDI greater than 1.5.³⁶⁻³⁸ We attributed the uncontrolled

polymerization to a radical formation through oxidation reaction of the amine or glycidyl group by EY. In this study, we demonstrate that EY did not interfere with the various functional groups as demonstrated by a good agreement between the theoretical and experimental molecular weights assessed by GPC. All the polymers have been prepared with a PDI lower than 1.3, which confirms a living character. UV-vis spectroscopy after purification confirmed the presence of dithioester by the signal at $\lambda = 305\text{nm}$ ($\epsilon = 15\,100\text{ M}^{-1}\text{ cm}^{-1}$) (data not shown). Using Bert-Lambert equation, the end group functionality was determined to be greater than 95% for all the polymers. At the end of the polymerization, EY was completely eliminated by precipitation as demonstrated by the absence of signal at 539 nm ($\epsilon = 60\,803\text{ M}^{-1}\text{ cm}^{-1}$).³⁰



Scheme 3. Chemical structures of monomers employed in this study. GMA, HEMA, MMA, OEGMA, DMAEMA, PFPMA, MAA and HPMA stand for glycidyl methacrylate, hydroxyethyl methacrylate, methyl methacrylate, oligoethylene glycol methylether methacrylate, *N,N*-dimethylaminoethyl methacrylate, pentafluorophenyl methacrylate, methacrylic acid and hydroxylpropyl methacrylamide.

Table 3. Polymerizations of methyl methacrylate (MMA) mediated by eosin Y and eosin Y/TEA as photoredox catalysts in the absence or presence of oxygen.

No.	$[\text{MMA}]/[\text{CPADB}]/[\text{eosin Y}]/[\text{TEA}]^a$	Nitrogen	Time (h)	Conv. ^b (%)	$M_{n, \text{theo.}}^c$ (g/mol)	$M_{n, \text{GPC}}^d$ (g/mol)	M_w/M_n^d
1	200/0/0.02/0	Yes	24	5	-	250 000	3.8
2	200/0/0.02/0	No	24	0	-	-	-
3	200/0/0.02/0.1	Yes	24	9	-	203 000	3.2
4	200/0/0.02/0.1	No	24	0	-	-	-
5	200/1/0/1	Yes	24	7	1680	3 020	1.26
6	200/1/0/1	No	24	0	-	-	-
7	200/1/0.02/0	Yes	12	52	10 670	11 400	1.14
8	200/1/0.02/0	No	12	24	5 100	6 530	1.18
9	200/1/0.02/1	Yes	12	67	13 610	14 100	1.20
10	200/1/0.02/1	No	12	73	14 920	15 130	1.21

Note: a) The reactions were performed in DMSO at room temperature under 4.8 W blue LED light ($\lambda_{\text{max}} = 435\text{ nm}$); b) Monomer conversion determined by ¹H NMR spectroscopy; c) Theoretical molecular weight calculated using the following equation: $M_{n, \text{th.}} = [\text{M}]_0/[\text{CPADB}]_0 \times \text{MW}^M \times \alpha$ (NMR) + MW^{CPADB} , where $[\text{M}]_0$, $[\text{Thiocar.}]_0$, MW^M , α (NMR) and MW^{CPADB} correspond to monomer and thiocarbonylthio compound concentration, molar mass of monomer, conversion measured by NMR and molar mass of CPADB compound respectively; d) Molecular weight and polydispersity determined by GPC using universal calibration.

Subsequently, we investigated the polymerization of OEGMA in different solvents, including acetonitrile (MeCN), toluene, water, DMSO and *N,N*-dimethylformamide (DMF) using $[\text{OEGMA}]:[\text{CPADB}]:[\text{EY}]$ molar ratio of 200:1:0.01 under blue LED light (4.8W) to demonstrate the versatility of this polymerization technique. At different time points, aliquots were taken from the polymerization mixture and were analysed by GPC and NMR. For all these solvents, except toluene, we observed a linear relationship between $\ln([\text{M}]_0/[\text{M}])$ and the exposure time. The solvents had strong effect on the apparent propagation rate. DMSO and water gave the fastest polymerization rates, while the polymerizations performed in MeCN and DMF presented slow polymerization kinetics (**Figure 2**). Interestingly, we did not observe monomer conversion in toluene after 24 hours of irradiation. One of the explanations is that EY is quenched in toluene. Except the polymerizations performed in toluene, the evolutions of the molecular weights were in good agreement with the theoretical ones, which demonstrate that EY can be an efficient photoredox catalyst for PET-RAFT in polar solvents (**Figure 2B**). In our previous work employing metal photocatalysts *fac*-

$[\text{Ir}(\text{ppy})_3]$ and $\text{Ru}(\text{bpy})_3\text{Cl}_2$,^{36,37} PET-RAFT technique was proved to be extremely tolerant to oxygen. We decided to investigate if EY has the ability to perform polymerization in the presence of oxygen. **Figure 3A** indicated a linear plot of $\ln([\text{M}]_0/[\text{M}])$ versus exposure time for both systems, i.e., in the absence and presence of oxygen. However, the polymerization in the presence of oxygen presented a lower apparent propagation rate, k_p^{app} , 0.027 h^{-1} than that in the absence of oxygen ($k_p^{\text{app}} = 0.070\text{ h}^{-1}$). The result obtained for polymerization in the presence of oxygen suggested that a fraction of EY was used to activate CPADB, while the other fraction was employed to consume O_2 to form superoxide anions. Interestingly, both systems presented the same induction periods which suggested that the electron transfer from excited state EY^* to CPADB and oxygen can occur concurrently. The proposed reaction pathway was shown in **Scheme 2A**. At the end of the polymerization, the polymers were purified by precipitation in methanol and analysed by NMR and UV-vis to determine the presence of dithiobenzoate. In the presence and absence of oxygen, NMR and UV-vis revealed high end group fidelity ($f > 95\%$).

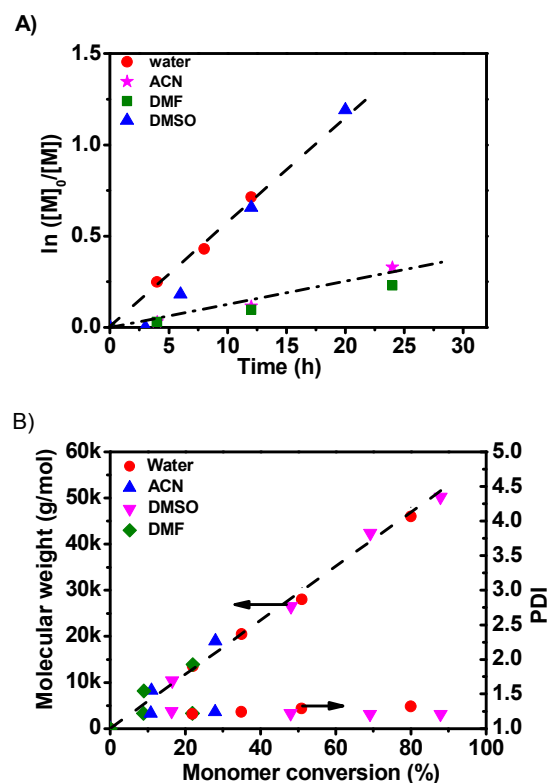


Figure 2. A) Evolution of $\ln([M]_0/[M]_t)$ vs. exposure time for PET-RAFT polymerization of OEGMA mediated by eosin Y (EY) in various solvents using CPADB as thiocarbonylthio compound (50 ppm of EY in respect to monomer); B) Evolution of molecular weight and PDI vs. exposure time for PET-RAFT polymerization of OEGMA mediated by eosin Y (EY) in various solvents using CPADB as thiocarbonylthio compound (50 ppm of EY relative to monomer).

Table 4. Polymerizations of functional monomers mediated by eosin Y as photoredox catalysts.

#	Monomer ^a	Time (h)	Conv. (%) ^b	$M_{n, \text{theo.}}$ (g/mol) ^c	$M_{n, \text{GPC}}$ (g/mol) ^d	PDI^d
1	HEMA	12	55	14 500	15 200	1.21
2	DMAEMA	12	69	21 900	22 500	1.18
3	PFPMA	12	56	28 500	29 600	1.14
4	MAA	12	51	8 900	10 200	1.36
5	HPMA	12	75	22 500	12 800 (23 500) ^e	1.18
6	GMA	12	58	16 700	16 900	1.16
7	OEGMA	12	60	36 300	34 500	1.22

Note: a) The reactions were performed using $[Monomer]/[eosin\ Y]/[CPADB]$ ratio of 200/0.02/1 in DMSO at room temperature under 4.8 W blue LED light ($\lambda_{\text{max}} = 435\ \text{nm}$); b) Monomer conversion determined by ^1H NMR spectroscopy; c) Theoretical molecular weight calculated using the following equation: $M_{n, \text{th.}} = [M]_0/[Thiocar.]_0 \times MW^M \times \alpha^{(NMR)} + MW^{Thiocar.}$, where $[M]_0$, $[Thiocar.]_0$, MW^M , $\alpha^{(NMR)}$ and $MW^{Thiocar.}$ correspond to monomer and thiocarbonylthio compound concentration, molar mass of monomer, conversion measured by NMR and molar mass of thiocarbonylthio compound respectively; d) Molecular weight and polydispersity determined by GPC, e) molecular weight determined by NMR.

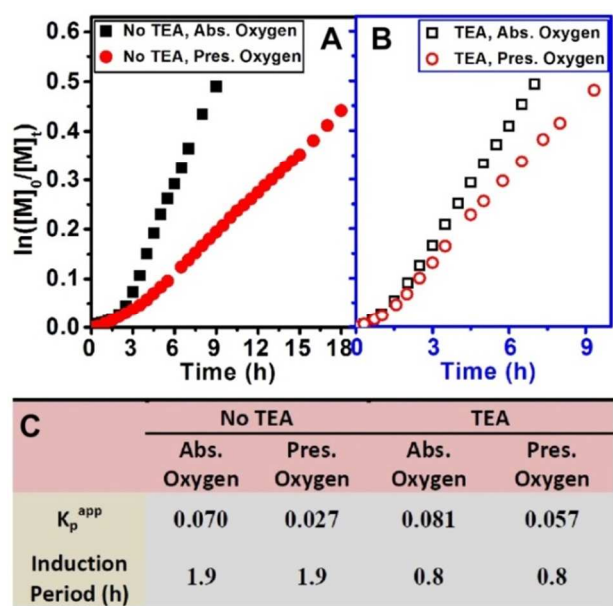


Figure 3. Kinetic study for PET-RAFT polymerization of MMA mediated by eosin Y (EY) or EY/TEA in the absence or presence of oxygen. (A) $\ln([M]_0/[M]_t)$ versus exposure time using $[MMA]:[CPADB]:[EY] = 200 : 1 : 0.02$; (B) $\ln([M]_0/[M]_t)$ versus exposure time using $[MMA]:[CPADB]:[EY]:[TEA] = 200 : 1 : 0.02 : 0.1$; (C) kinetic data table for k_p^{app} and induction periods. Notes: The reactions were performed in DMSO at room temperature under 4.8 W blue LED light ($\lambda_{\text{max}} = 435\ \text{nm}$).

Recent work in organic synthesis^{26, 30} and polymer synthesis^{32, 35} using EY in the presence of air suggests that the addition of triethylamine (TEA) improves the reaction yield. For instance, Bowman and co-workers demonstrate the use of EY in the presence of TEA to initiate a free radical polymerization under light.^{32, 35} TEA is an excellent reducing agent,⁴⁵⁻⁴⁷ capable to act as a sacrificial agent which provides an electron to EY to yield EY⁻. As shown in **Scheme 2B**, EY acts as an electron carrier. Such mechanism has been described previously for several organic reactions using metallo- and organo- photocatalysts.^{25, 48} Therefore, the polymerization rate in the presence of TEA should be greater in the presence of oxygen. We decided to test this assumption by the addition of a small amount of TEA in our previous reaction (i.e., $[CPADB]/[TEA] = 1/0.1$). In the presence of TEA, it was evident that the apparent propagation rates increased slightly in the absence of oxygen, whereas the polymerization rate was doubled in the presence of oxygen (**Figure 3B**). In addition, the induction periods was surprisingly reduced from 1.9 hours to 0.8 of an hour when the polymerization was performed under air, which demonstrated that TEA was capable of effectively improving oxygen consumption.

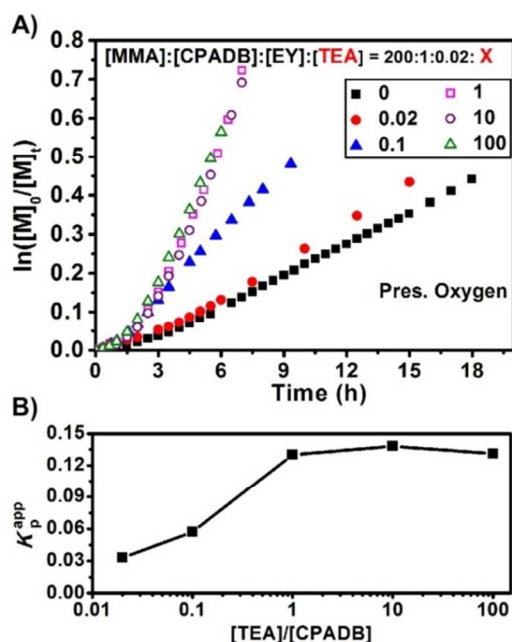


Figure 4. Effects of TEA concentration on the kinetics of PET-RAFT polymerization of MMA mediated by eosin Y in the presence of oxygen.

Inspired by early work using TEA and EY for organic synthesis,^{25, 30} we proposed another mechanism to describe PET-RAFT in the presence of TEA. In the presence of an electron donor, such as TEA, reductive pathway is privileged instead of oxidative pathway (Scheme 2A/B).^{26, 27} In this pathway, an electron transfer from the electron donor (TEA) to EY is initiated with the formation of amine radical cation, $\text{Et}_3\text{N}^{\cdot+}$, as shown in Scheme 2B, to generate EY radical anion ($\text{EY}^{\cdot-}$). The radical cation ($\text{Et}_3\text{N}^{\cdot+}$) derived from the oxidation of triethylamine can react with a second molecule of TEA or solvents by hydrogen abstraction to yield inactive species.^{47, 49-53} In the presence of oxygen, one part of $\text{EY}^{\cdot-}$ will reduce oxygen to generate superoxide ($\text{O}_2^{\cdot-}$), whereas the other fraction of $\text{EY}^{\cdot-}$ will transfer an electron to CPADB to generate a propagating radicals for chain growth. As a control experiment, we performed the polymerization of MMA without CPADB in the presence of EY and TEA ([Eosin]:[TEA] = 0.02:0.1) under air and nitrogen. In this condition, we observed a very low monomer conversion (<10%, Table 2, #3-4) after 24 hours which indicates that CPADB plays an important role in the activation of the polymerization.

However, the amount of TEA (1.65×10^{-3} mmol) present in the FTNIR reaction vessel using a molar ratio of [TEA]:[CPADB] = 0.1/1 was insufficient to completely reduce the dissolved oxygen and free oxygen in the reactor vessel (i.e., 2.48×10^{-3}

mmol, see experimental section in ESI). Thus, we decided to increase the amount of TEA and investigate its effect on the photo-polymerization rates, as shown in Figure 4. Firstly, it is interesting to note that there was a great effect of TEA concentrations on the propagation rates in the presence of oxygen, whereas very little difference was observed in the absence of oxygen (Table S1 in ESI). Monomer conversions were determined to be 11 and 42% after 6 hours of light irradiation when the polymerization is carried with a [TEA]:[CPADB] ratio of 0 and 1, respectively. Kinetic data for different molar ratios of TEA, [MMA]:[CPADB]:[EY]:[TEA] = 200: 1 : 0.02 : (0~100), were plotted in Figure 4A. The polymerization rates increased when the [TEA]:[CPADB] ratio varies from 0 to 1, while for a TEA molar ratio greater than 1, the apparent polymerization rates remained constant (Figure 4B). These results could be depicted with the proposed mechanism in Scheme 2B.

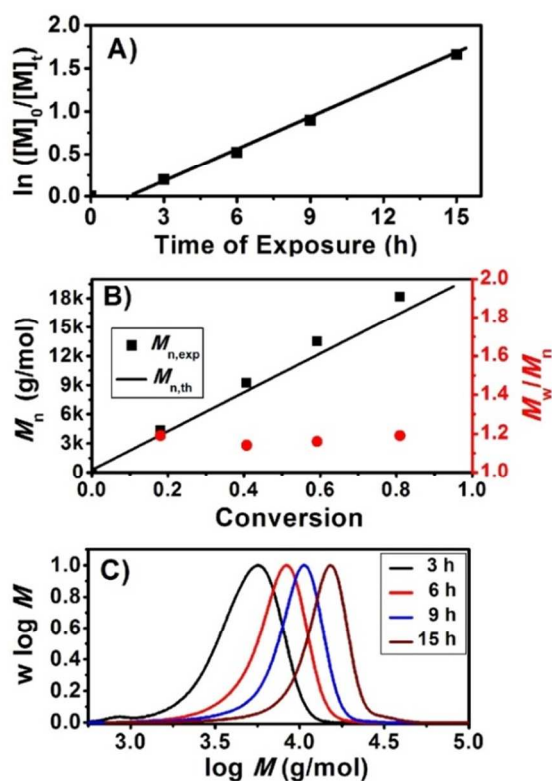


Figure 5. PET-RAFT polymerization of MMA mediated by eosin Y (EY)/triethylamine (TEA) in DMSO using CPADB as thiocarbonylthio compound: A) $\ln([M]_0/[M]_t)$ vs. time of exposure; B) molecular weights and M_w/M_n vs. conversion; C) molecular weight distributions of PMMA at different time points. Note: The reactions were performed in DMSO at room temperature under 4.8 W blue LED light ($\lambda_{\text{max}} = 435$ nm) using [MMA]:[CPADB]:[EY]:[TEA] = 200 : 1 : 0.02 : 1 in the presence of oxygen.

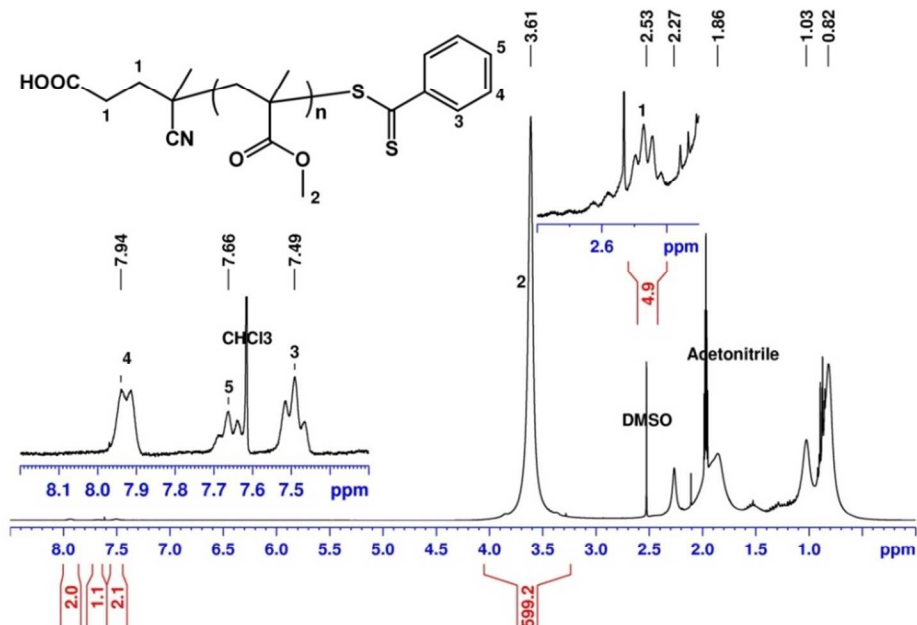


Figure 6. ^1H NMR spectrum (CD_3CN) for purified PMMA prepared by PET-RAFT polymerization mediated by EY/TEA in the presence of oxygen. Note: The peak of CHCl_3 and DMSO is attributed to the solvents used for polymerization and dissolution. $M_{n,\text{NMR}} = 20\,250$ g/mol, $M_{n,\text{GPC}} = 21\,710$ g/mol, $M_w/M_n = 1.09$.

In a second part of this paper, we sought to investigate the polymerization kinetics of MMA in the presence of TEA and oxygen (**Figure 5**). The measured molecular weights were in good agreement with theoretical ones, whilst the polydispersity values stayed lower than 1.3 over the polymerization period. The retention of the dithiobenzoate end-group was confirmed by different techniques. GPC equipped with a dual RI-UV detector showed that the molecular weight distributions obtained by UV ($\lambda = 305\text{nm}$) and RI detectors were in good agreement (**Figure S2** in ESI). ^1H NMR analysis (**Figure 6**) revealed the presence of dithiobenzoate at 7.49, 7.66 and 7.94 ppm, while UV-vis spectroscopy (**Figure S3** in ESI) showed the characteristic signal at 305nm. In order to demonstrate the presence of end group fidelity, successful chain extensions of PMMA were performed to yield diblock copolymers PMMA-*b*-PMMA (**Figure S4** in ESI) and PMMA-*b*-POEGMA (**Figure S6** in ESI). The absence of shoulder at low molecular weight confirmed the preservation of RAFT end group during RAFT polymerization. The composition of final diblock copolymers was confirmed by ^1H NMR (**Figures S5 and S7** in ESI).

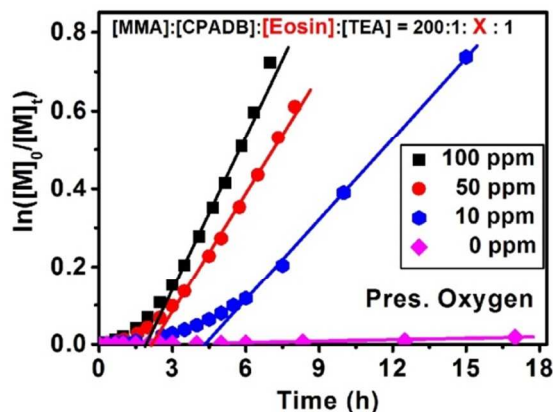
Having successfully demonstrated the specific role of TEA in PET-RAFT polymerization, we directed our efforts to the effects of EY concentration on polymerization kinetics in the presence of oxygen (**Figure 7**). Here, we fixed the

concentration of TEA, MMA and CPADB and we varied the concentration of EY from 0 to 100ppm. An increase in apparent propagation rates was observed with increasing EY concentrations in the presence of oxygen. The induction periods were greatly decreased as well, which was attributed to the fast activation of RAFT agent and rapid consumption of oxygen. **Figure 7** shows that the photocatalyst concentration could be reduced to 50ppm in the presence of oxygen which offers an acceptable polymerization rate (50% monomer conversion in less than 6 hours). In addition, the PDI decreased from 1.19 to 1.14 when the amount of EY was decreased from 100 to 10ppm.

Conclusions

Visible light-mediated controlled/"living" radical polymerization via photoinduced electron transfer-reversible addition-fragmentation chain transfer (PET-RAFT) mechanism could utilize organic photocatalysts, such as eosin Y or fluorescein, to yield well-defined (co)polymers with controlled molecular weights and polydispersities. The addition of triethylamine allowed to perform the polymerization under oxygen (without the need for degassing). Triethylamine acts as a sacrificing electron donor to reduce oxygen in the polymerization system. In addition, the EY can activate the

polymerization of functional monomers, including glycidyl methacrylate, 2-hydroxyl ethyl methacrylate, pentafluorophenylacetate ester methacrylate and *N,N*-dimethylaminoethyl methacrylate. Finally, we have optimized the concentration of EY and triethylamine to yield well defined polymers under air.



EY Conc. (ppm to monomer)	$K_p^{app.}$	Induction Period (h)	Data for final polymers		
			$M_{n,exp}$	$M_{n,theo}$	PDI
0	0.0013	4.4	2 000	1 080	1.35
10	0.068	4.2	10 290	10 980	1.14
50	0.11	2.4	9 540	9 790	1.15
100	0.14	2.1	10 350	11010	1.19

Figure 7. PET-RAFT polymerization of MMA mediated by TEA using various concentration of eosin Y (EY) (100, 50, 10, and 0 ppm relative to MMA) in the presence of oxygen. Note: the reactions were performed in DMSO at room temperature under 4.8 W blue LED light ($\lambda_{max} = 435$ nm).

Acknowledgements

The authors thank UNSW for funding (SPF01). CB acknowledges Australian Research Council (ARC) for his Future Fellowship (ARC – FT 1210096).

Notes and references

^aCentre for Advanced Macromolecular Design (CAMD) and Australian Centre for NanoMedicine (ACN), School of Chemical Engineering, UNSW Australia, Sydney, NSW 2052, Australia
E-mail: cboyer@unsw.edu.au; j.xu@unsw.edu.au.

[†]Electronic Supplementary Information (ESI) available: [Figures S1-S7, Table S1 and other characterizations]. See DOI: 10.1039/b000000x/

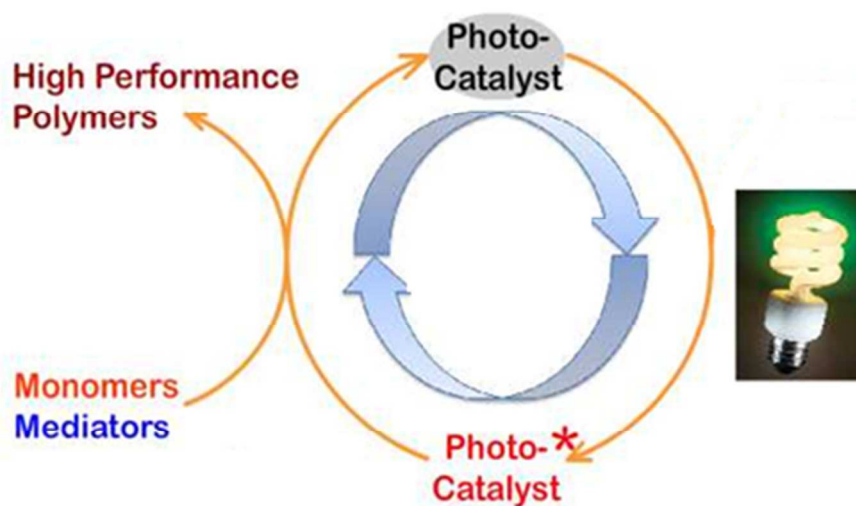
1. J. E. Poelma, B. P. Fors, G. F. Meyers, J. W. Kramer and C. J. Hawker, *Angew. Chem. Inter. Ed.*, 2013, **52**, 6844-6848.
2. B. P. Fors, J. E. Poelma, M. S. Menyo, M. J. Robb, D. M. Spokoiny, J. W. Kramer, J. H. Waite and C. J. Hawker, *J. Am. Chem. Soc.*, 2013, **135**, 14106-14109.
3. F. D. Jochum and P. Theato, *Chem. Soc. Rev.*, 2013, **42**, 7468-7483.
4. B. P. Fors and C. J. Hawker, *Angew. Chem. Inter. Ed.*, 2012, **51**, 8850-8853.

5. F. A. Leibfarth, K. M. Mattson, B. P. Fors, H. A. Collins and C. J. Hawker, *Angew. Chem. Inter. Ed.*, 2013, **52**, 199-210.
6. D. Konkolewicz, K. Schröder, J. Buback, S. Bernhard and K. Matyjaszewski, *ACS Macro Lett.*, 2012, **1**, 1219-1223.
7. Y. Kwak and K. Matyjaszewski, *Macromolecules*, 2010, **43**, 5180-5183.
8. A. Anastasaki, V. Nikolaou, Q. Zhang, J. Burns, S. R. Samanta, C. Waldron, A. J. Haddleton, R. McHale, D. Fox, V. Percec, P. Wilson and D. M. Haddleton, *J. Am. Chem. Soc.*, 2014, **136**, 1141-1149.
9. M. A. Tasdelen, M. Ciftci and Y. Yagci, *Macro. Chem. Phys.*, 2012, **213**, 1391-1396.
10. A. Anastasaki, V. Nikolaou, A. Simula, J. Godfrey, M. Li, G. Nurumbetov, P. Wilson and D. M. Haddleton, *Macromolecules*, 2014, **47**, 3852-3859.
11. B. Wenn, M. Conradi, A. D. Carreiras, D. M. Haddleton and T. Junkers, *Polym. Chem.*, 2014, **5**, 3053-3060.
12. M. Ciftci, M. A. Tasdelen and Y. Yagci, *Polym. Chem.*, 2014, **5**, 600-606.
13. T. G. Ribelli, D. Konkolewicz, S. Bernhard and K. Matyjaszewski, *J. Am. Chem. Soc.*, 2014.
14. Y. Zhao, M. Yu, S. Zhang, Y. Liu and X. Fu, *Macromolecules*, 2014.
15. T. G. Ribelli, D. Konkolewicz, X. Pan and K. Matyjaszewski, *Macromolecules*, 2014.
16. N. J. Treat, B. P. Fors, J. W. Kramer, M. Christianson, C.-Y. Chiu, J. R. d. Alaniz and C. J. Hawker, *ACS Macro Lett.*, 2014, **3**, 580-584.
17. D. A. Nicewicz and D. W. C. MacMillan, *Science*, 2008, **322**, 77-80.
18. C. K. Prier, D. A. Rankic and D. W. C. MacMillan, *Chem. Rev.*, 2013, **113**, 5322-5363.
19. T. P. Yoon, M. A. Ischay and J. Du, *Nat Chem*, 2010, **2**, 527-532.
20. J. M. R. Narayanam and C. R. J. Stephenson, *Chem. Soc. Rev.*, 2011, **40**, 102-113.
21. J. W. Tucker and C. R. J. Stephenson, *J. Org. Chem.*, 2012, **77**, 1617-1622.
22. C.-J. Wallentin, J. D. Nguyen, P. Finkbeiner and C. R. J. Stephenson, *J. Am. Chem. Soc.*, 2012, **134**, 8875-8884.
23. Z. Lu and T. P. Yoon, *Angew. Chem. Inter. Ed.*, 2012, **51**, 10329-10332.
24. D. Ravelli, M. Fagnoni and A. Albini, *Chem. Soc. Rev.*, 2013, **42**, 97-113.
25. M. Majek, F. Filace and A. J. v. Wangelin, *Beilstein J. Org. Chem.*, 2014, **10**, 981-989.
26. D. A. Nicewicz and T. M. Nguyen, *ACS Catalysis*, 2013, **4**, 355-360.
27. D. Ravelli and M. Fagnoni, *ChemCatChem*, 2012, **4**, 169-171.
28. A. A. Waheed and P. D. Gupta, *J. Biochem. Biophys. Methods*, 1996, **33**, 187-196.
29. P. Meallier, S. Guittonneau, C. Emmelin and T. Konstantinova, *Dyes and Pigments*, 1999, **40**, 95-98.
30. D. P. Hari and B. Konig, *Chem. Comm.*, 2014, **50**, 6688-6699.
31. J. Zhang, L. Sun and T. Yoshida, *J. Electroanalytical Chem.*, 2011, **662**, 384-395.
32. H. J. Avens, T. J. Randle and C. N. Bowman, *Polymer*, 2008, **49**, 4762-4768.
33. S. Kizilel, V. H. Pérez-Luna and F. Teymour, *Langmuir*, 2004, **20**, 8652-8658.
34. M. Farsari, G. Filippidis, K. Sambani, T. S. Drakakis and C. Fotakis, *J. Photochem. Photobio. A: Chem.*, 2006, **181**, 132-135.
35. H. J. Avens and C. N. Bowman, *J. Polym. Sci. Part A: Polym. Chem.*, 2009, **47**, 6083-6094.
36. a) J. Xu, K. Jung, A. Atme, S. Shanmugam and C. Boyer, *J. Am. Chem. Soc.*, 2014, **136**, 5508-5519; b) J. Xu, K. Jung, N. A. Corrigan and C. Boyer, *Chem. Sci.*, 2014, **5**, 3568-3575.
37. a) S. Shanmugam, J. Xu and C. Boyer, *Macromolecules*, 2014, **47**, 4930-4942; b) J. Xu, K. Jung and C. Boyer, *Macromolecules*, 2014, **47**, 4217-4229.
38. C. Fu, J. Xu, L. Tao and C. Boyer, *ACS Macro Lett.*, 2014, **3**, 633-638.
39. C. Boyer, A. Granville, T. P. Davis and V. Bulmus, *J. Polym. Sci. Part A: Polym. Chem.*, 2009, **47**, 3773-3794.

Journal Name

40. J. Xu, L. Tao, C. Boyer, A. B. Lowe and T. P. Davis, *Macromolecules*, 2010, **44**, 299-312.
41. G. R. Fleming, A. W. E. Knight, J. M. Morris, R. J. S. Morrison and G. W. Robinson, *J. Am. Chem. Soc.*, 1977, **99**, 4306-4311.
42. M. Asha Jhonsi, A. Kathiravan and R. Renganathan, *J. Mol. Struct.*, 2009, **921**, 279-284.
43. L. Bahadur and P. Srivastava, *Solar Energy Materials and Solar Cells*, 2003, **79**, 235-248.
44. a) D. Magde, R. Wong and P. G. Seybold, *Photochem. Photobio.*, 2002, **75**, 327-334; b) D. L. Sackett and J. Wolff *Anal. Biochem.* 1987, **167**, 228-234.
45. H. D. Burrows, *Photochem. Photobio.*, 1974, **19**, 241-243.
46. J. Perez-Prieto, R. E. Galian, M. C. Morant-Minana and M. A. Miranda, *Chem. Comm.*, 2006, 1021-1023.
47. P. J. DeLaive, T. K. Foreman, C. Giannotti and D. G. Whitten, *J. Amer. Chem. Soc.*, 1980, **102**, 5627-5631.
48. J. Hu, J. Wang, T. H. Nguyen and N. Zheng, *Beilstein J. Org. Chem.*, 2013, **9**, 1977-2001.
49. C. D. Russell, *Anal. Chem.*, 1963, **35**, 1291-1292.
50. S. G. Cohen, A. Parola and G. H. Parsons, *Chem. Rev.*, 1973, **73**, 141-161.
51. P. J. DeLaive, C. Giannotti and D. G. Whitten, *J. Am. Chem. Soc.*, 1978, **100**, 7413-7415.
52. D. Behar, T. Dhanasekaran, P. Neta, C. M. Hosten, D. Ejeh, P. Hambright and E. Fujita, *J. Phys. Chem. A*, 1998, **102**, 2870-2877.
53. J. Grodkowski, D. Behar, P. Neta and P. Hambright, *J. Phys. Chem. A*, 1997, **101**, 248-254.
54. B. Karagoz, C. Boyer and T. P. Davis, *Macro. Rapid Comm.*, 2014, **35**, 417-421.
55. J. Jose and K. Burgess, *J. Org. Chem.*, 2006, **71**, 7835-7839.

TOC



In this work, we demonstrate the use of organophotoredox catalyst under visible to perform photoinduced electron transfer – reversible addition fragmentation chain transfer (PET-RAFT) for the polymerization of methacrylate monomers.